Contribution from the Department of Chemistry,
Purdue University, West Lafayette, Indiana 47907

Bis(diphenylphosphino)methane Complexes of the Multiply Bonded Ditungsten(III) Core. Structure of $W_2(\mu\text{-H})(\mu\text{-Cl})Cl_4(\mu\text{-dppm})_2$

Phillip E. Fanwick, William S. Harwood, and Richard A. Walton*

Received July 1, 1986

The blue-green ditungsten(III) complex $W_2(\mu\text{-H})(\mu\text{-Cl})Cl_4(dppm)_2$ (**1**) (dppm = $Ph_2PCH_2PPh_2$) is formed in the reactions between $W_2Cl_4(P\text{-}n\text{-}Bu_3)_4$ and dppm in toluene and between $W_2(mhp)_4$ (mhp is the monoanion of 2-hydroxy-6-methylpyridine), Me_3SiCl, and dppm in methanol. When CH_3OD is used as the solvent in the latter reaction, the deuteride $W_2(\mu\text{-D})(\mu\text{-Cl})Cl_4(dppm)_2$ is formed. Crystals of **1** were grown from the toluene reaction mixture. This complex crystallizes in the monoclinic space group $P2_1/c$, with the following unit cell dimensions: a = 17.549 (3) Å, b = 12.633 (2) Å, c = 21.661 (3) Å, β = 93.07 (1)°, V = 4795 (2) Å^3, and Z = 4. The structure was refined to R = 0.051 (R_w = 0.080) for 4424 data with $F^2 > 3.0\sigma(F^2)$. The structure is best described as an edge-shared bioctahedron in which there is a short W-W distance of 2.4830 (9) Å, consistent with some degree of metal-metal multiple bonding. The dppm ligands assume the usual intramolecular bridging mode and are in a trans relationship to one another. The reaction between $W_2Cl_6(THF)_4$ and dppm in THF affords the diamagnetic complex $W_2(\mu\text{-Cl})_2Cl_4(dppm)_2$ (**2**). The dark red-brown salts $[W_2(\mu\text{-Cl})_2Cl_3(dppm)_2(CNR)]PF_6$ (**3**) are formed when **1** is reacted with isocyanide ligands RNC (R = mesityl, xylyl, *tert*-butyl) in 1,2-dichloroethane in the presence of the one-electron oxidant $[(\eta^5\text{-}C_5H_5)_2Fe]PF_6$. These contain a terminally bound RNC ligand and are believed to bear a close structural relationship to **2**. The spectroscopic and electrochemical properties of **1-3** have been examined in considerable detail.

Introduction

We have recently been examining those reactions of the multiply bonded complexes $Re_2(\mu\text{-dppm})_2X_4$ (X = Cl, Br; dppm = bis(diphenylphosphino)methane) and $Mo_2(\mu\text{-dppm})_2X_4$ (X = Cl, Br, I) with the π-acceptor isocyanide (RNC) and CO ligands in which a dinuclear unit is preserved in the products. Examples include the A-frame-like complexes $Re_2(\mu\text{-X})X_3(\mu\text{-dppm})_2L$ (L = RNC, CO),[1-4] the bis(isocyanide) complex $[Re_2Cl_3(\mu\text{-dppm})_2(CN\text{-}t\text{-}Bu)_2]PF_6$,[2,5] the mixed isocyanide-carbonyl complex $Re_2(\mu\text{-Cl})(\mu\text{-CO})Cl_3(\mu\text{-dppm})_2(CNxyl)$,[4] and the dimolybdenum(II) species $[Mo_2Cl_3(\mu\text{-dppm})_2(CNR)]PF_6$ (R = *i*-Pr, *t*-Bu).[6] The extension of this chemistry to the analogous ditungsten(II) complex $W_2(\mu\text{-dppm})_2Cl_4$ has necessitated the design of a synthetic route to this compound. Schrock and co-workers[7] have outlined a synthesis for complexes of the type $W_2Cl_4(LL)_2$ (LL = $R_2PCH_2CH_2PR_2$ where R = Me, Et, or Ph) by substitution of these bidentate ligands for the monodentate phosphines in $W_2Cl_4(P\text{-}n\text{-}Bu_3)_4$. Such a procedure, when applied to the synthesis of $W_2Cl_4(\mu\text{-dppm})_2$, gives the ditungsten(III) complex $W_2(\mu\text{-H})(\mu\text{-Cl})Cl_4(\mu\text{-dppm})_2$. This surprising result has led us to examine the properties and structure of this interesting complex. Comparisons are made with the chemistry of the related ditungsten(III) complex of stoichiometry $W_2Cl_6(dppm)_2$, which we have also prepared for the first time in this work.

Experimental Section

Starting Materials. The compounds $W_2Cl_4(PR_3)_4$ (PR_3 = PMe_3, P-*n*-Pr_3, P-*n*-Bu_3, PMe_2Ph, $PMePh_2$),[7] $W_2Cl_6(THF)_4$,[7] $W_2(mhp)_4$ (mhp is the monoanion of 2-hydroxy-6-methylpyridine),[8] *tert*-butyl isocyanide (*t*-BuNC),[9] 2,4,6-trimethylphenyl isocyanide (mesNC)[9] and $[(\eta^5\text{-}C_5H_5)_2Fe]PF_6$[10] were prepared as reported in the literature. Samples of 2,6-dimethylphenyl isocyanide (xylNC), purchased from Fluka AG, and dppm, purchased from Strem Chemicals, were used without further purification. All solvents were reagent grade and were deoxygenated prior to use. Reactions were performed under an atmosphere of dry nitrogen.

A. Synthesis of $W_2(\mu\text{-H})(\mu\text{-Cl})Cl_4(dppm)_2$ (1). Method 1. A 25-mL flask was charged with 0.35 g (0.27 mmol) of $W_2Cl_4(P\text{-}n\text{-}Bu_3)_4$, 0.217 g (0.565 mmol) of dppm, and 10 mL of toluene. The solution was gently refluxed in the presence of a pine boiling stick for 12 h and then cooled slowly (4-6 h) to room temperature. Blue crystals separated from solution and deposited on the boiling stick. These were collected (in air), washed with toluene followed by diethyl ether, and then vacuum-dried; yield 0.176 g (50%). Anal. Calcd for $C_{50}H_{45}Cl_5P_4W_2$: C, 45.67; H, 3.46; Cl, 13.48. Found: C, 45.15; H, 3.65; Cl, 13.41.

Method 2. A 50-mL three-neck flask was charged with 0.30 g (0.37 mmol) of $W_2(mhp)_4$, 0.29 g (0.76 mmol) of dppm, 4.0 mL of methanol, and 0.40 mL (5.1 mmol) of Me_3SiCl. The reaction mixture was stirred at room temperature for 2 h and then filtered under nitrogen. The blue-green precipitate was washed with methanol and then vacuum-dried; yield 0.24 g (50%). The spectroscopic and electrochemical properties of this product were identical with those found for the complex formed by using method 1.

B. $W_2(\mu\text{-D})(\mu\text{-Cl})Cl_4(dppm)_2$. This compound was synthesized in a manner very similar to that described for method 2 in part A but with CH_3OD in place of CH_3OH; yield 74%. It was identified by a comparison of its IR spectrum and electrochemical properties to those of the hydride.

C. Synthesis of $W_2Cl_6(dppm)_2$ (2). A 100-mL three-neck flask was filled with dry nitrogen and charged with 1.47 g (4.51 mmol) of WCl_4, 40 mL of freshly distilled THF, and 0.107 g (4.66 mmol) of sodium amalgam. The suspension was stirred at room temperature for 3 h and allowed to settle. The reaction mixture was filtered under nitrogen into a flask equipped with a reflux condenser, and the insoluble residue was washed with THF. The volume of the combined yellow-green filtrate and washings was reduced under vacuum to approximately 40 mL, 1.85 g (4.82 mmol) of dppm was added, and the solution was brought to reflux for 30 min and then stirred at room temperature for 24 h. The orange precipitate was collected by filtration, washed with THF, and vacuum-dried; yield 1.53 g (50%, based on WCl_4). Anal. Calcd for $C_{50}H_{44}Cl_6P_4W_2$: C, 44.51; H, 3.29; Cl, 15.77. Found: C, 44.44; H, 3.59; Cl, 15.74.

D. Reactions of $W_2(\mu\text{-H})(\mu\text{-Cl})Cl_4(dppm)_2$ with Isocyanides. (a) $[W_2(\mu\text{-Cl})_2Cl_3(dppm)_2(CNmes)]PF_6$ (3a). A 50-mL round-bottom flask was charged with 0.24 g (0.18 mmol) of $W_2(\mu\text{-H})(\mu\text{-Cl})Cl_4(dppm)_2$ and 0.12 g (0.81 mmol) of mesNC (which was dissolved in a minimum volume of diethyl ether), and this mixture was then treated with 25 mL of 1,2-dichloroethane. The suspension was refluxed for 36 h and cooled to room temperature, and then 0.064 g (0.19 mmol) of $[(\eta^5\text{-}C_5H_5)_2Fe]PF_6$ was added. Stirring of the reaction mixture was continued for 1 h. It was then filtered in air and the filtrate evaporated under a stream of dry nitrogen. The residue was dissolved in a minimum volume of acetone, and the mixture was filtered to remove any unreacted $W_2(\mu\text{-H})(\mu\text{-Cl})Cl_4(dppm)_2$. The filtrate was layered under diethyl ether (75 mL), and after slow diffusion of the solvent layers had taken place, the compound was collected as a fine powder; yield 0.22 g (78%). The sample for

(1) Cotton, F. A.; Daniels, L. M.; Dunbar, K. R.; Falvello, L. R.; Tetrick, S. M.; Walton, R. A. *J. Am. Chem. Soc.* **1985**, *107*, 3524.
(2) Anderson, L. B.; Barder, T. J.; Walton, R. A. *Inorg. Chem.* **1985**, *24*, 1421.
(3) Anderson, L. B.; Barder, T. J.; Esjornson, D.; Walton, R. A.; Bursten, B. E. *J. Chem. Soc., Dalton Trans.*, in press.
(4) Cotton, F. A.; Dunbar, K. R.; Price, A. C.; Schwotzer, W.; Walton, R. A. *J. Am. Chem. Soc.* **1986**, *108*, 4843.
(5) Anderson, L. B.; Barder, T. J.; Cotton, F. A.; Dunbar, K. R.; Falvello, L. R.; Walton, R. A. *Inorg. Chem.* **1986**, *25*, 3629.
(6) Harwood, W. S.; Qi, J.-S.; Walton, R. A. *Polyhedron* **1986**, *5*, 15.
(7) Schrock, R. R.; Sturgeoff, L. G.; Sharp, P. R. *Inorg. Chem.* **1983**, *22*, 2801.
(8) Cotton, F. A.; Fanwick, P. E.; Niswander, R. H.; Sekutowski, J. C. *J. Am. Chem. Soc.* **1978**, *100*, 4725.
(9) Weber, W. D.; Gokel, G. W.; Ugi, I. K. *Angew. Chem., Int. Ed. Engl.* **1972**, *11*, 530.
(10) Hendrickson, C. N.; Soh, Y. S.; Gray, H. B. *Inorg. Chem.* **1971**, *10*, 1559.

0020-1669/87/1326-0242$01.50/0

Table I. Crystallographic Data and Data Collection Parameters for $W_2(\mu\text{-H})(\mu\text{-Cl})Cl_4(dppm)_2$[a]

formula	$W_2Cl_5P_4C_{50}H_{45}$
fw	1314.8
space gp	$P2_1/c$
a, Å	17.549 (3)
b, Å	12.633 (2)
c, Å	21.661 (3)
β, deg	93.07 (1)
V, Å^3	4795 (2)
Z	4
d_{calcd} g cm^{-3}	1.807
cryst dimens, mm	0.34 × 0.16 × 0.08
temp, °C	23.0
radiation (wavelength, Å)	Mo Kα (0.710 73)
monochromater	graphite
linear abs coeff, cm^{-1}	53.08
abs corr applied	empirical[b]
diffractometer	Enraf-Nonius CAD4
scan method	θ–2θ
h, k, l limits	−18 to +18, 0 to +13, 0 to +23
2θ range, deg	4.00–45.00
scan width, deg	0.85 + 0.35 tan θ
takeoff angle, deg	5.00
programs used	Enraf-Nonius SDP
F_{000}	2548.0
unique data	6238
data with $I > 3.0\sigma(I)$	4424
no. of variables	550
largest shift/esd in final cycle	0.13
R[c]	0.051
R_w[d]	0.080
goodness of fit[e]	2.014

[a] Numbers in parentheses following certain data are estimated standard deviations occurring in the least significant digit. [b] Walker, N.; Stuart, D. *Acta Crystallogr., Sect. A Found Crystallogr.* **1983**, *A39*, 158. [c] $R = \sum||F_o| - |F_c||/\sum|F_o|$. [d] $R_w = [\sum w(|F_o| - |F_c|)^2/\sum w|F_o|^2]^{1/2}$; $w = 1/\sigma^2(F_o)$. [e] Goodness of fit = $[\sum w(|F_o| - |F_c|)^2/(N_{observns} - N_{params})]^{1/2}$.

microanalysis was recrystallized from CH_2Cl_2/pentane. Anal. Calcd for $C_{60}H_{55}Cl_5F_6NP_5W_2$: C, 44.93; H, 3.46; Cl, 11.05. Found: C, 44.87; H, 3.59; Cl, 11.31.

(b) $[W_2(\mu\text{-Cl})_2Cl_3(dppm)_2(CNxyl)]PF_6$ (3b). The synthesis of this compound was similar to that for **3a**; yield 73%. Anal. Calcd for $C_{59}H_{53}Cl_5F_6NP_5W_2$: C, 44.57; H, 3.37; Cl, 11.15. Found: C, 44.20; H, 3.69; Cl, 11.18.

(c) $[W_2(\mu\text{-Cl})_2Cl_3(dppm)_2(CN\text{-}t\text{-}Bu)]PF_6\cdot C_3H_6O$ (3c). The synthesis of this compound was similar to that for **3a**; yield 78%. Anal. Calcd for $C_{58}H_{59}Cl_5F_6NOP_5W_2$: C, 43.54; H, 3.72; Cl, 11.08. Found: C, 43.94; H, 3.83; Cl, 11.24. IR spectral measurements (Nujol mull) showed ν(CO) = 1709 cm^{-1} for the lattice acetone.

Preparation of Single Crystals of $W_2(\mu\text{-H})(\mu\text{-Cl})Cl_4(\mu\text{-dppm})_2$. The general procedure used was similar to that described above in method 1. However, a solution volume of 30 mL was used, and no boiling stick was present. The reaction mixture was maintained at 90 °C for 36 h and then cooled over the course of 12 h to room temperature. The crystals obtained were large, and they were doubled in such a way that two single crystals shared a face. The crystals could easily be separated and cut to the appropriate size.

X-ray Structure Determination. A large crystal was cut with a razor, and the resulting fragment, which had dimensions 0.34 × 0.16 × 0.08 mm, was mounted on a glass fiber with epoxy cement. The crystal was indexed, and data were collected on an Enraf-Nonius CAD-4 diffractometer equipped with a graphite monochromater and a standard-focus molybdenum X-ray tube. Crystal data and information relating to data collection and structure refinement are listed in Table I. Three standard reflections were measured after every hour of beam exposure during data collection and displayed no systematic variation in intensity. Further details of the crystal data collection and reduction methods are available elsewhere.[11]

Calculations were performed on a PDP 11/34 computer using the Enraf-Nonius structure determination package. The structure was refined in the monoclinic space group $P2_1/c$. An empirical absorption correction was applied.[12] The linear absorption coefficient was 53.08 cm^{-1}. No correction for extinction was applied. The least-squares program minimized the function $w(|F_o| - |F_c|)^2$, where the weighting factor $w = 1/\sigma^2(F_o)$. All atoms were refined anisotropically, and corrections for anomalous scattering were applied to all atoms.[13] Hydrogen atoms were not included in the final least-squares refinement. The final residuals were $R = 0.051$ and $R_w = 0.080$, and the final difference Fourier map displayed no peaks of chemical significance. The bridging hydride ligand was not located in this structure analysis, but its presence can be inferred on the basis of spectroscopic and magnetic properties (vide infra). Further details concerning the data set, the structure solution, and the structure refinement may be obtained from Dr. P. E. Fanwick. Table II lists the atomic positional parameters and their errors, while Table III lists selected intramolecular bond distances and angles. A listing of thermal parameters (Table S1) and complete listings of bond distances (Table S2) and bond angles (Table S3) are available as supplementary material, as well as a figure (Figure S1) that shows the full atomic numbering scheme.

Physical Measurements. Infrared spectra were recorded as Nujol mulls between KBr plates with an IBM Instruments IR 32 Fourier transform (4000–400 cm^{-1}) spectrometer. In this region from 500 to 50 cm^{-1}, spectra were measured by using polyethylene plates and a Digilab FTS-20B FTIR spectrometer. Electronic absorption spectra of dichloromethane solutions were recorded on IBM Instruments 9420 (900–300 nm) and Cary 17 (1800–900 nm) UV–visible spectrophotometers. Electrochemical measurements were carried out on dichloromethane solutions that contained 0.1 M tetra-*n*-butylammonium hexafluorophosphate (TBAH) as supporting electrolyte. $E_{1/2}$ values, determined as $(E_{p,a} + E_{p,c})/2$, were referenced to the silver/silver chloride (Ag/AgCl) electrode at room temperature and are uncorrected for junction potentials. Voltammetric experiments were performed by using a Bioanalytical Systems Inc. Model CV-1A instrument in conjunction with a Hewlett-Packard Model 7035B X-Y recorder. X-Band ESR spectra were obtained with the use of a Varian E-109 spectrometer. $^{31}P\{^1H\}$ NMR spectra were recorded on a Varian XL-200 spectrometer operated at 80.98 MHz and using an internal deuterium lock and 85% H_3PO_4 as an external standard. Positive chemical shifts were measured downfield from H_3PO_4. ^1H NMR spectra were obtained on a Varian XL-200 spectrometer. Resonances were referenced internally to the impurity in the deuteriated solvent.

Analytical Procedures. Elemental microanalyses were performed by Dr. H. D. Lee of the Purdue University microanalytical laboratory.

Results and Discussion

(a) Synthesis and Spectroscopic and Electrochemical Properties of $W_2(\mu\text{-H})(\mu\text{-Cl})Cl_4(dppm)_2$ (1). The most surprising feature of the reaction between $W_2Cl_4(P\text{-}n\text{-}Bu_3)_4$ and dppm in hot toluene is that oxidation to a W_2^{6+} derivative occurs so readily. While the formation of this particular hydrido species in such a nonhydridic medium demonstrates the propensity of the quadruply bonded W_2^{4+} core to undergo a net two-electron oxidation, it stands in contrast to other examples, such as the formation of $[W_2(\mu\text{-H})(\mu\text{-Cl})_2Cl_6]$[13-14] and $W_2(\mu\text{-H})(\mu\text{-Cl})Cl_2(O_2CPh)_2(P\text{-}n\text{-}Bu_3)_2$,[15] where this oxidation occurs in an acidic (HX) medium. While we do not know for certain the mechanism by which **1** is formed from $W_2Cl_4(P\text{-}n\text{-}Bu_3)_4$ in toluene, we note that the ditungsten(II) complex $W_2Cl_4(dppm)_2$ has recently been isolated from such a reaction mixture.[16]

A more logical synthetic procedure for **1** involves the reaction of $W_2(mhp)_4$ (mhp is the monoanion of 2-hydroxy-6-methylpyridine)[8] with dppm and Me_3SiCl in methanol, a method that can also be used to prepare the deuteride $W_2(\mu\text{-D})(\mu\text{-Cl})Cl_4(dppm)_2$ when methanol-d_1 is used as the reaction solvent. It is most likely that the hydroxy proton is the source of the hydride ligand. This synthetic route was first suggested to us by Professor R. E. McCarley, who has utilized such a method to prepare the

(11) Fanwick, P. E.; Harwood, W. S.; Walton, R. A. *Inorg. Chim. Acta*, in press.

(12) Walker, N.; Stuart, D. *Acta Crystallogr., Sect. A: Found Crystallogr.* **1983**, *A39*, 158.

(13) (a) Cromer, D. T. *International Tables for X-ray Crystallography*; Kynoch: Birmingham, England, 1974; Vol. IV, Table 2.3.1. (b) For the scattering factors used in the structure solution see: Cromer, D. T.; Waber, J. T. *Ibid.*, Table 2.2B.

(14) Sattelberger, A. P.; McLaughlin, K. W.; Huffman, J. C. *J. Am. Chem. Soc.* **1981**, *103*, 2880.

(15) Cotton, F. A.; Mott, G. N. *J. Am. Chem. Soc.* **1982**, *104*, 5978.

(16) Cotton, F. A.; Canich, J., unpublished results.

Table II. Positional Parameters and Equivalent Isotropic Displacement Parameters for Non-Hydrogen Atoms and Their Estimated Standard Deviations[a]

atom	x	y	z	B, Å²	atom	x	y	z	B, Å²
W(1)	0.25933 (4)	0.08326 (5)	0.11385 (3)	2.38 (1)	C(1211)	0.1708 (9)	0.217 (1)	0.2491 (8)	2.8 (3)
W(2)	0.25489 (4)	−0.09626 (5)	0.16020 (3)	2.34 (1)	C(1212)	0.173 (1)	0.244 (1)	0.3147 (8)	4.0 (4)
P(11)	0.2752 (2)	0.0196 (3)	0.0039 (2)	2.47 (8)	C(1213)	0.107 (1)	0.272 (1)	0.3391 (8)	3.7 (4)
P(12)	0.2603 (3)	0.1842 (4)	0.2157 (2)	2.77 (9)	C(1214)	0.038 (1)	0.275 (1)	0.3049 (9)	4.3 (4)
P(21)	0.2523 (3)	−0.1948 (3)	0.0575 (2)	2.62 (9)	C(1215)	0.036 (1)	0.249 (2)	0.2415 (9)	4.3 (4)
P(22)	0.2686 (3)	−0.0320 (4)	0.2727 (2)	2.76 (9)	C(1216)	0.103 (1)	0.221 (2)	0.2116 (9)	4.6 (5)
Cl(11)	0.1832 (3)	0.2267 (3)	0.0669 (2)	3.8 (1)	C(2111)	0.1622 (9)	−0.221 (1)	0.0131 (7)	2.7 (3)
Cl(12)	0.3781 (3)	0.1681 (4)	0.1047 (2)	4.0 (1)	C(2112)	0.165 (1)	−0.244 (1)	−0.0486 (7)	3.0 (4)
Cl(21)	0.3698 (2)	−0.1927 (4)	0.1801 (2)	3.5 (1)	C(2113)	0.098 (1)	−0.268 (1)	−0.0831 (8)	3.9 (4)
Cl(22)	0.1730 (3)	−0.2368 (4)	0.1982 (2)	3.7 (1)	C(2114)	0.029 (1)	−0.267 (1)	−0.054 (1)	4.5 (5)
Cl(B)	0.1348 (3)	−0.0017 (3)	0.1321 (2)	3.51 (9)	C(2115)	0.026 (1)	−0.241 (2)	0.0097 (9)	4.2 (4)
C(B1)	0.3126 (9)	−0.117 (1)	0.0060 (7)	2.8 (3)	C(2116)	0.093 (1)	−0.218 (1)	0.0419 (7)	3.4 (4)
C(B2)	0.312 (1)	0.100 (1)	0.2746 (7)	3.3 (4)	C(2121)	0.295 (1)	−0.327 (1)	0.0556 (8)	3.8 (4)
C(1111)	0.3469 (9)	0.093 (1)	−0.0382 (7)	2.8 (4)	C(2122)	0.249 (1)	−0.416 (1)	0.0687 (8)	4.1 (4)
C(1112)	0.414 (1)	0.045 (1)	−0.0546 (7)	3.5 (4)	C(2123)	0.279 (2)	−0.515 (1)	0.065 (1)	6.4 (6)
C(1113)	0.466 (1)	0.112 (2)	−0.0858 (9)	4.9 (5)	C(2124)	0.353 (1)	−0.529 (2)	0.051 (1)	7.0 (6)
C(1114)	0.454 (1)	0.212 (2)	−0.0974 (9)	5.3 (5)	C(2125)	0.402 (1)	−0.444 (2)	0.038 (1)	6.2 (6)
C(1115)	0.385 (1)	0.260 (2)	−0.0757 (8)	5.0 (5)	C(2126)	0.369 (1)	−0.341 (2)	0.041 (1)	5.7 (5)
C(1116)	0.334 (1)	0.202 (1)	−0.0466 (8)	3.9 (4)	C(2211)	0.187 (1)	−0.017 (1)	0.3218 (7)	2.9 (4)
C(1121)	0.1958 (9)	0.014 (1)	−0.0548 (6)	2.3 (3)	C(2212)	0.202 (1)	0.006 (1)	0.3854 (7)	4.1 (4)
C(1122)	0.209 (1)	−0.010 (1)	−0.1171 (7)	3.4 (4)	C(2213)	0.142 (1)	0.028 (2)	0.4210 (9)	4.6 (5)
C(1123)	0.149 (1)	−0.029 (1)	−0.1594 (7)	3.4 (4)	C(2214)	0.066 (1)	0.025 (2)	0.3961 (9)	5.3 (5)
C(1124)	0.074 (1)	−0.026 (2)	−0.1437 (9)	5.0 (5)	C(2215)	0.050 (1)	0.001 (1)	0.3310 (9)	4.8 (5)
C(1125)	0.059 (1)	0.001 (1)	−0.0782 (7)	3.5 (4)	C(2216)	0.113 (1)	−0.023 (1)	0.2951 (7)	3.2 (4)
C(1126)	0.121 (1)	0.023 (1)	−0.0361 (6)	2.7 (3)	C(2221)	0.335 (1)	−0.113 (1)	0.3213 (7)	3.2 (4)
C(1221)	0.311 (1)	0.311 (1)	0.2236 (7)	3.3 (4)	C(2222)	0.405 (1)	−0.072 (2)	0.344 (1)	5.3 (5)
C(1222)	0.270 (2)	0.401 (2)	0.218 (1)	6.6 (7)	C(2223)	0.453 (1)	−0.141 (2)	0.383 (1)	5.9 (6)
C(1223)	0.312 (1)	0.501 (1)	0.222 (1)	6.5 (6)	C(2224)	0.435 (1)	−0.247 (2)	0.3844 (9)	5.9 (5)
C(1224)	0.388 (1)	0.501 (2)	0.2381 (8)	5.7 (5)	C(2225)	0.368 (1)	−0.287 (1)	0.3563 (7)	3.5 (4)
C(1225)	0.431 (1)	0.410 (2)	0.2459 (9)	5.4 (5)	C(2226)	0.316 (1)	−0.217 (1)	0.3249 (7)	3.1 (4)
C(1226)	0.390 (1)	0.312 (2)	0.2370 (9)	4.8 (5)					

[a] Anisotropically refined atoms are given in the form of the isotropic equivalent thermal parameter defined as follows: $(4/3)[a^2B(1,1) + b^2B(2,2) + c^2B(3,3) + ab(\cos\gamma)B(1,2) + ac(\cos\beta)B(1,3) + bc(\cos\alpha)B(2,3)]$.

Table III. Some Important Bond Distances (Å) and Angles (deg) for $W_2(\mu\text{-H})(\mu\text{-Cl})Cl_4(dppm)_2$[a]

A. Bond Distances

W(1)–W(2)	2.4830 (9)	W(2)–P(21)	2.548 (4)
W(1)–P(11)	2.544 (4)	W(2)–P(22)	2.567 (4)
W(1)–P(12)	2.547 (4)	W(2)–Cl(21)	2.375 (4)
W(1)–Cl(11)	2.441 (5)	W(2)–Cl(22)	2.453 (5)
W(1)–Cl(12)	2.362 (5)	W(2)–Cl(B)	2.470 (4)
W(1)–Cl(B)	2.486 (5)		

B. Bond Angles

W(2)–W(1)–P(11)	95.6 (1)	W(1)–W(2)–P(21)	95.3 (1)
W(2)–W(1)–P(12)	96.1 (1)	W(1)–W(2)–P(22)	95.3 (1)
W(2)–W(1)–Cl(11)	144.9 (1)	W(1)–W(2)–Cl(21)	119.8 (1)
W(2)–W(1)–Cl(12)	119.7 (1)	W(1)–W(2)–Cl(22)	145.9 (1)
W(2)–W(1)–Cl(B)	59.6 (1)	W(1)–W(2)–Cl(B)	60.2 (1)
P(11)–W(1)–P(12)	166.7 (1)	P(21)–W(2)–P(22)	168.4 (1)
P(11)–W(1)–Cl(11)	85.9 (1)	P(21)–W(2)–Cl(21)	83.3 (1)
P(11)–W(1)–Cl(12)	85.6 (1)	P(21)–W(2)–Cl(22)	87.4 (1)
P(11)–W(1)–Cl(B)	98.8 (1)	P(21)–W(2)–Cl(B)	92.6 (1)
P(12)–W(1)–Cl(11)	88.2 (1)	P(22)–W(2)–Cl(21)	87.4 (1)
P(12)–W(1)–Cl(12)	83.1 (2)	P(22)–W(2)–Cl(22)	86.4 (1)
P(12)–W(1)–Cl(B)	92.5 (1)	P(22)–W(2)–Cl(B)	96.7 (1)
Cl(11)–W(1)–Cl(12)	95.4 (2)	Cl(21)–W(2)–Cl(22)	94.3 (2)
Cl(11)–W(1)–Cl(B)	85.4 (2)	Cl(21)–W(2)–Cl(B)	175.9 (1)
Cl(12)–W(1)–Cl(B)	175.5 (2)	Cl(22)–W(2)–Cl(B)	85.7 (1)
		W(1)–Cl(B)–W(2)	60.1 (1)

[a] Numbers in parentheses are estimated standard deviations in the least significant digits.

related species $W_2(\mu\text{-H})(\mu\text{-Cl})Cl_4L_4$ (L = pyridine, 4-ethylpyridine),[17] which are close structural analogues of **1**.

The chloro analogue of **1**, viz. $W_2Cl_6(dppm)_2$ (**2**), is prepared by the reaction of $W_2(\mu\text{-Cl})_2Cl_4(THF)_4$ with dppm. While we have been unable to grow single crystals of **2** that are suitable for an X-ray crystal structure analysis, it in all likelihood possesses a structure similar to that of compounds of the type $M_2(\mu\text{-Cl})_2Cl_4(\mu\text{-}R_2PCH_2PR_2)_2$ (M = Nb, Ta, Mo, Re, Ru; R = Me, Ph).[18,19]

The most convincing spectroscopic evidence for **1** being a hydrido species is provided by IR spectroscopy. Its Nujol mull spectrum shows a feature at 1614 m-w cm^{-1}, which shifts to 1160 cm^{-1} upon deuteriation. While the latter band overlaps that of a dppm absorption, it is nonetheless easily discernible. This shift matches that found in the IR spectra of $W_2(\mu\text{-H})(\mu\text{-Cl})Cl_4L_4$ and $W_2(\mu\text{-D})(\mu\text{-Cl})Cl_4L_4$ (L = py, 4-Etpy).[17] In the low-frequency Nujol mull IR spectra of **1** and **2**, bands attributable to ν(W–Cl) are seen at 325 s, 305 s, and 276 m cm^{-1} and at 338 s, 305 s, and 276 m cm^{-1}, respectively. The features at 276 cm^{-1} are probably due to the bridging modes $\nu(W\text{–}Cl_b\text{–}W)$.[20]

The electronic absorption spectrum of **1** [λ_{max}, nm (ϵ): 1012 (340), 790 (220), 602 (450), 464 (460), 386 (3300)] for a solution in CH_2Cl_2 matches quite closely the reflectance spectra of $W_2(\mu\text{-H})(\mu\text{-Cl})Cl_4L_4$ (L = py, 4-Etpy), which have λ_{max} ~900, ~700, ~580, and ~460 nm.[17] These spectral features in turn resemble somewhat those seen in the spectrum of a CH_2Cl_2 solution of **2**, which has the following bands [λ_{max}, nm (ϵ)]: 822 (740), 641 (285), 468 (4800), 387 (3200). The latter complex, which is diamagnetic, is a member of a growing series of complexes of stoichiometry $M_2Cl_6(R_2PCH_2PR_2)_2$.

The results of extended Hückel calculations for $[W_2(\mu\text{-Cl})_2Cl_8]^{4-}$ are in good agreement with the conclusion of Shaik et al.[21] and Cotton et al.[22] for other $M_2(\mu\text{-Cl})_2Cl_8$ type molecules.[23]

(17) Carlin, R. T.; McCarley, R. E., unpublished results.

(18) Chakravarty, A. R.; Cotton, F. A.; Diebold, M. P.; Lewis, D. B.; Roth, W. J. *J. Am. Chem. Soc.* **1986**, *108*, 971.
(19) Barder, T. J.; Cotton, F. A.; Lewis, D.; Schwotzer, W.; Tetrick, S. M.; Walton, R. A. *J. Am. Chem. Soc.* **1984**, *106*, 2882.
(20) (a) Nakamoto, K. *Infrared and Raman Spectra of Inorganic and Coordination Compounds*, 3rd ed.; Wiley: New York, 1978; pp 163–171 and references cited therein. (b) Walton, R. A.; Brisdon, B. J. *Spectrochim. Acta, Part A* **1967**, *23A*, 2489.
(21) Shaik, S.; Hoffmann, R.; Fisel, C. R.; Summerville, R. H. *J. Am. Chem. Soc.* **1980**, *102*, 4555 and references therein.

The Walsh diagram for $[W_2(\mu\text{-}Cl)_2Cl_8]^{4-}$ exhibits the general feature of δ^* below δ for all bond lengths and W–Cl_b–W angles. This is due to the interaction of the filled p orbitals of the bridging halide with the metal d_{xy} orbitals.[21] Accordingly, the ground-state electronic configuration can be represented as $\sigma^2\pi^2\delta^{*2}$, a description that may also be relevant to $W_2(\mu\text{-}H)(\mu\text{-}Cl)Cl_4(dppm)_2$ although this is by no means certain. The expected diamagnetism of **1** is supported by a magnetic suceptibility measurement that gave $\chi_g = -0.29 \times 10^{-6}$ cgsu as determined by the Faraday method.[24,25] Furthermore, although **1** is not very soluble in CD_2Cl_2 and related solvents, we were able to obtain a sharp well-defined ^1H NMR (470-MHz) spectrum. These observations support the formulation of **1** as a derivative of W_2^{6+} and not the paramagnetic W_2^{5+} core. The phenyl protons on the dppm ligand are seen as multiplets at δ +7.78, +7.33, and +7.24. The methylene resonances appear somewhat downfield from the usual values found in $Mo_2Cl_4(dppm)_2$ (δ +4.35)[6] and $W_2Cl_6(dppm)_2$ (vide infra). They appear as an AB pattern (displaying no observable ^{31}P–^1H coupling) at δ +6.14 (d) and +4.55 (d) with $^2J_{AB}$ = 12.9 Hz. The observation of an AB pattern is indicative of the absence of a plane of symmetry that contains the W_2P_4 unit; this suggests that the solution structure of **1** is the same as that observed in the solid state (vide infra). Unfortunately, we were unable to locate the resonance for the unique bridging hydrido ligand. This is probably a consequence of the weakness of the signal because of the poor solubility properties of **1**, broadening of the signal due to coupling to the ^{31}P nuclei and/or obscuring of the signal because of overlap with dppm resonances. This problem is compounded by the difficulty of predicting where this resonance will occur; for example, W–*H* resonances for the monohydrides $W_2(\mu\text{-}H)(\mu\text{-}Cl)Cl_2(O_2CPh)_2(P\text{-}n\text{-}Bu_3)_2$,[15] $W_2(\mu\text{-}H)(\mu\text{-}Cl)Cl_2(hp)_2(P\text{-}n\text{-}Bu_3)_2$ (hp is the monoanion of 2-hydroxypyridine),[26] $[W_2(\mu\text{-}H)Cl_6(\mu\text{-}Me_2S)_2]^-$,[27] and $[W_2(\mu\text{-}H)(\mu\text{-}OCH_2\text{-}t\text{-}Bu)_2(OCH_2\text{-}t\text{-}Bu)_6]^-$[28] occur at δ +1.92 (doublet of doublets), −0.82 (doublet of doublets), +3.60, and ca. +9, respectively.

The more soluble complex **2** exhibits a ^1H NMR spectrum (in CD_2Cl_2) with phenyl resonances (multiplets) centered at ca. δ +7.4 and +7.2 and a singlet for the $-CH_2-$ resonance of dppm at δ +3.51 with no evidence of coupling to the ^{31}P nuclei. In this case we have also recorded the $^{31}P\{^1H\}$ spectrum (in CD_2Cl_2)—this displays a broad singlet at δ −96, which is shifted upfield (to lower frequency) from free dppm (δ −22.7 in CH_2Cl_2 solution vs. 85% H_3PO_4). This high-field shift and broadening of the ^{31}P resonance are consistent with the thermal population of a low-lying paramagnetic state at room temperature. Under these conditions nuclear relaxation effects could be expected to quench ^{31}P–^1H coupling.[29] Such an effect has been seen previously in the spectrum of $Re_2(\mu\text{-}Cl)_2Cl_4(dppm)_2$.[19]

Both **1** and **2** display a quite rich redox chemistry. The cyclic voltammogram of **1** in 0.1 M TBAH–CH_2Cl_2 exhibits two reversible processes at $E_{1/2}$ = −0.85 V and $E_{1/2}$ = −1.68 V vs. Ag/AgCl, both of which correspond to one-electron reductions of the bulk complex (Figure 1a). For both couples, the $i_{p,a}/i_{p,c}$ ratios were close to unity and the separation between the coupled anodic and cathodic peaks (ΔE_p) was ca. 100 mV at v = 200 mV/s. For the couple at $E_{1/2}$ = −0.85 V, the $i_p/v^{1/2}$ ratio was essentially constant for sweep rates (v) between 50 and 400 mV/s. These properties are (with this solvent system and our cell configuration) consistent with an electron-transfer process that approaches reversibility.[30] Controlled-potential electrolysis at −1.0 V generated solutions that contained the orange monoanion along with small amounts of decomposition products. Reoxidation of these solutions at −0.7 V regenerated **1**. For **1**, there are also two oxidations at $E_{p,a}$ = +0.69 and +1.14 V vs. Ag/AgCl, neither of which is reversible, although the former appears to become more reversible (the $i_{p,c}/i_{p,a}$ ratio approached unity) if a switching

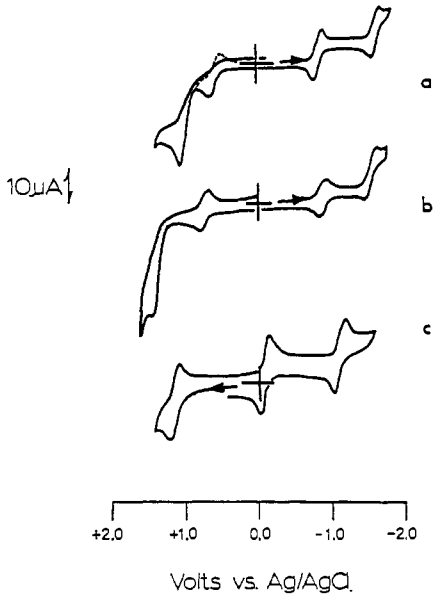

Figure 1. Single-scan cyclic voltammograms of (a) $W_2(\mu\text{-}H)(\mu\text{-}Cl)Cl_4(dppm)_2$, (b) $W_2(\mu\text{-}Cl)_2Cl_4(dppm)_2$, and (c) $[W_2(\mu\text{-}Cl)_2Cl_3(dppm)_2(CNxy)]PF_6$ in 0.1 M TBAH–CH_2Cl_2 (v = 200 mV/s; a Pt-bead electrode). In the case of (a), the dashed line represents the appearance of the couple at ca. +0.7 V when a switching potential of ca. +0.9 V is used.

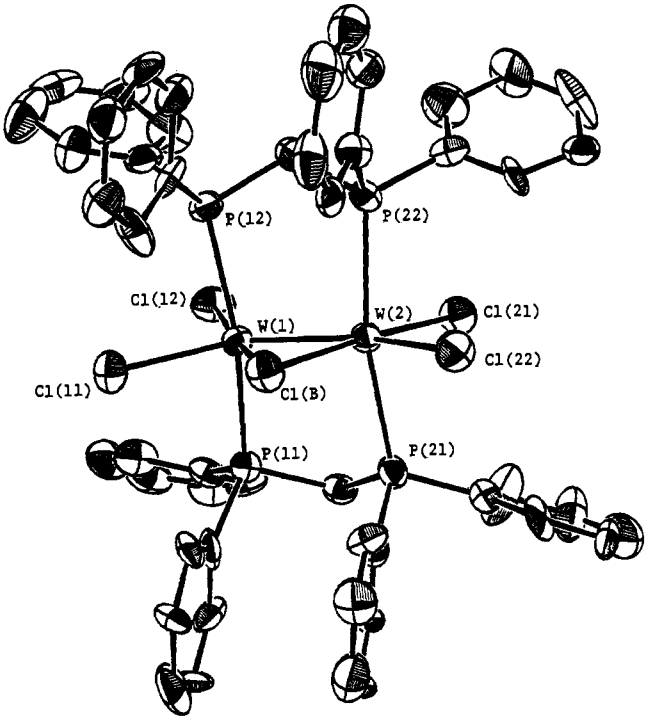

Figure 2. ORTEP view of $W_2(\mu\text{-}H)(\mu\text{-}Cl)Cl_4(dppm)_2$ (bridging hydride omitted). Thermal ellipsoids are drawn at the 50% probability level.

(22) Cotton, F. A.; Diebold, M. P.; O'Connor, C. J.; Powell, G. L. *J. Am. Chem. Soc.* **1985**, *107*, 7438.
(23) We thank Mr. Jiali Gao for help with these calculations.
(24) These measurements were carried out for us by Professor T. J. Smith of Kalamazoo College.
(25) The X-band ESR spectrum of frozen deoxygenated CH_2Cl_2 solutions of **1** (−160 °C) showed weak features at g = 1.88, 1.82, and 1.74. These resonances are attributed to small quantities of a paramagnetic impurity; upon electrochemical oxidation of these solutions, complex **1** decomposed and the observed ESR signals increased in intensity as the amount of impurity increased.
(26) Harwood, W. S.; Walton, R. A., unpublished results.
(27) Boorman, P. M.; Moynihan, K. J.; Kerr, K. A. *J. Chem. Soc., Chem. Commun.* **1981**, 1286.
(28) Chisholm, M. H.; Huffman, J. C.; Smith, C. A. *J. Am. Chem. Soc.* **1986**, *108*, 222.
(29) La Mar, G. N.; Horrocks, W. DeW, Jr.; Holm, R. H., Eds. *NMR of Paramagnetic Molecules*; Academic: New York, 1973; p 566.
(30) Zietlow, T. C.; Klendworth, D. D.; Nimry, T.; Salmon, D. J.; Walton, R. A. *Inorg. Chem.* **1981**, *20*, 947.

Table IV. Spectroscopic and Electrochemical Properties of $[W_2(\mu\text{-Cl})_2Cl_3(dppm)_2(CNR)]PF_6$ (R = mes, xyl, *t*-Bu)

compd	IR spectra[a]		electr abs spectra[b]	^{1}H NMR, δ[c]		^{31}P NMR, δ[e]	half-wave potentials[d]		
	ν(C≡N)	ν(W—Cl)	λ, nm (ε)	$-CH_2-$[e]	$-CH_3$[f]		$E_{1/2}$ (1)	$E_{1/2}$ (2)	$E_{1/2}$ (3)
3a, R = mes	2166 vs	322 sh, 312 s, 296 m, 280 w, 267 w	1494 (200), 1080 (550), 762 (820), 475 (6300)	3.72 d, 3.29 d, ($^2J_{AB}$ = 13.3 Hz)	2.89 s, 2.42 s	−44 s, −95 s	+1.20 (ox)	−0.12 (red)	−1.17 (red)
3b, R = xyl	2170 vs	325 m, 309 s, 295 sh, 278 w, 267 w	1500 (340), 1085 (900), 761 (800), 482 (5600)	3.70 d, 3.28 d ($^2J_{AB}$ = 13.7 Hz)	2.48 s	−47 s, −96 s	+1.19 (ox)	−0.10 (red)	−1.14 (red)
3c, R = *t*-Bu	2186 vs	*g*	*g*	3.88 d, 3.34 d, ($^2J_{AB}$ = 13.5 Hz)	1.03 s	*g*	+1.19 (ox)	−0.15 (red)	−1.24 (red)

[a] Nujol mull spectra on KBr plates (4000–400 cm^{-1}) or polyethylene plates (600–200 cm^{-1}). [b] Spectra recorded in CH_2Cl_2 (350–1800 nm); molar extinction coefficients given in parentheses. [c] Recorded in CD_2Cl_2 with ^{1}H NMR referenced to the residual protons of the solvent (δ +5.32); ^{31}P spectra referenced to 85% H_3PO_4. [d] Measured on 0.1 M TBAH–CH_2Cl_2 solutions by the cyclic voltammetric technique (V vs. Ag/AgCl); scan rate = 200 mV/s. [e] Resonances due to methylene protons of dppm ligand. [f] Resonances due to methyl protons of the isocyanide ligand. [g] Not measured.

potential of ca. +0.9 V is used (Figure 1a). In the case of **2**, its solutions in 0.1 M TBAH–CH_2Cl_2 possess a one-electron oxidation (by coulometry) at +0.79 V and a one-electron reduction at −0.91 V vs. Ag/AgCl (Figure 1b). Both of these processes approach reversibility, as judged by the electrochemical criteria mentioned above. If the electronic structure of **2** is correctly represented as $\sigma^2\pi^2\delta^{*2}$ (vide supra), then these two processes correspond to the generation of species (i.e., $\mathbf{2}^+$ and $\mathbf{2}^-$) that have the $\sigma^2\pi^2\delta^{*1}$ and $\sigma^2\pi^2\delta^{*2}\delta^1$ ground-state configurations, respectively. These possess W–W bonds of order 1.5 in each case. Additional redox processes are seen at $E_{p,a}$ = +1.5 V and $E_{p,c} \simeq -1.7$ V vs. Ag/AgCl in the cyclic voltammogram of **2** (Figure 1b), but these are both irreversible.

(b) Crystal Structure of $W_2(\mu\text{-H})(\mu\text{-Cl})Cl_4(dppm)_2$ (1). The pertinent structural data for **1** are listed in Tables I–III, and an ORTEP view of the molecule is shown in Figure 2. The dppm ligands adopt their usual intramolecular bridging mode with a transoid disposition to one another. Although we were unable to locate the single hydride ligand in this structure analysis, there is little doubt from chemical evidence that it is located in the open bridging position (Figure 2). Accordingly, **1** is best described as an edge-shared bioctahedron, like other species of the type $M_2(\mu\text{-X})_2X_4(\mu\text{-}R_2PCH_2PR_2)_2$.[18,19]

The W–W bond length of 2.4830 (9) Å is similar to the comparable distance found in the structure of $W_2(\mu\text{-H})(\mu\text{-Cl})Cl_4(4\text{-Etpy})_4$ (2.516 (2) Å),[17] although it is somewhat longer than for $W_2(\mu\text{-H})(\mu\text{-Cl})Cl_2(O_2CPh)_2(P\text{-}n\text{-}Bu_3)_2$ (2.423 (1) and 2.435 (1) Å for two independent molecules).[15] In any event, this distance is indicative of multiple-bond character in the W–W bond. Like these latter two structures, complex **1** has a W(μ-Cl)W unit that is almost an exact equilateral triangle. For the two terminal chloride ligands that are bound trans to the bridging chloride, the Cl_t–W–Cl_b angles approach linearity. The average W–Cl_t distance for these two W–Cl_t bonds is 2.369 [6] Å. This value is 0.078 Å less than the average W–Cl_t bond distance of 2.447 [6] Å for the chloride ligands cis to the bridge (i.e., that are trans to the hydride). Similar differences in W–Cl_t bond lengths are seen in the structures of $W_2(\mu\text{-H})(\mu\text{-Cl})Cl_2(O_2CPh)_2(P\text{-}n\text{-}Bu_3)_2$[15] and $W_2(\mu\text{-H})(\mu\text{-Cl})Cl_4(4\text{-Etpy})_4$.[17] The W–$Cl_b$ distance for **1** of 2.486 (4) Å is essentially the same as the comparable distance in both Cotton's compound[15] and McCarley's compound,[17] which in each instance is ca. 2.47 Å.

(c) Reactions of $W_2(\mu\text{-H})(\mu\text{-Cl})Cl_4(dppm)_2$ with Isocyanides. While the reactions of **1** with isocyanide ligands in 1,2-dichloroethane solvent do not afford pure products, in the presence of the one-electron oxidant $[(\eta^5\text{-}C_5H_5)_2Fe]PF_6$ we have isolated the dark red-brown complexes $[W_2Cl_5(dppm)_2(CNR)]PF_6$ [**3a–c** (R = mes, xyl, and *t*-Bu, respectively)]. In the absence of this oxidant, it appears that the RNC ligands reduce the ditungsten complex **1** to the neutral complex $W_2Cl_5(dppm)_2(CNR)$, but it is apparently not especially stable and we have not yet isolated it in an analytically pure form.

The diamagnetic compounds **3a–c** dissolve in acetonitrile to give solutions (ca. 10^{-3} M) that have conductivities (Λ_m = 149, 126, and 130 Ω^{-1} cm^2 mol^{-1}, respectively) that are in the range expected for 1:1 electrolytes (120–160 Ω^{-1} cm^2 mol^{-1}).[31] IR spectra (Nujol mull) of **3a–c** exhibit ν(C≡N) at 2166, 2170, and 2186 cm^{-1}, respectively (see Table IV). These values suggest that the isocyanide ligand is bound in a terminal fashion to the ditungsten unit. In the case of the low-frequency IR spectra, bands attributable[19] to ν(W–Cl_t) modes (those above ca. 290 cm^{-1}) and ν(W–Cl_b) modes (those below 290 cm^{-1}) are observed (see Table IV).

Key ^{1}H and ^{31}P{^{1}H} NMR (200-MHz) spectral data are summarized in Table IV. The $-CH_2-$ resonances of the dppm ligands are observed as an AB pattern with $^2J_{AB} \simeq 13.5$ Hz; there is no evidence of coupling to the phosphorus nuclei of dppm. This result is in keeping with a structure in which the molecule is unsymmetric about the W_2P_4 plane. We suggest that **3** has the following structure:

(31) Geary, W. J. *Coord. Chem. Rev.* **1971**, *7*, 81.

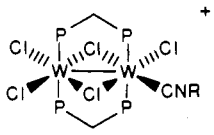

3 (R = mes, xyl, t-Bu)

Accordingly, species of this type can be viewed as substitution derivatives of **2**. The $^{31}P\{^1H\}$ resonances are broad and are shifted upfield from free dppm (δ -22.7).

The electrochemical properties of **3a-c** were studied by cyclic voltammetry (see Figure 1c). Data for solutions in 0.1 M TBAH-CH_2Cl_2 are summarized in Table IV. As mentioned earlier, compounds **3a-c** can be viewed as derivatives of $W_2Cl_6(dppm)_2$ (**2**), where a terminal chloride ligand has been substituted by an isocyanide. In related systems where substitution of halide by isocyanide has occurred, a shift of the electrochemical processes to more positive potentials is observed for the isocyanide complexes with respect to the original halide precursors.[6] For example, we see this type of shift in the case of $Mo_2X_4(dppm)_2$ (X = Cl, Br, I) upon conversion to the complexes $[Mo_2X_3(dppm)_2(CNR)]PF_6$ (R = *t*-Bu, *i*-Pr).[6] Thus, if we consider complexes **3a-c** as derivatives of $W_2Cl_6(dppm)_2$, then the two processes observed in the CV of the latter complex at $E_{1/2}(ox)$ = +0.79 V and $E_{1/2}(red)$ = -0.91 V vs. Ag/AgCl should shift to more positive potentials in the CV's of **3a-c**. In fact, the oxidation at +0.79 V for **2** shifts to +1.19 V (i.e. by 0.40 V to more positive potentials) while the reduction at -0.91 V in **2** shifts to -0.10 to -0.15 V (i.e. by 0.7-0.8 V to more positive potentials). In addition, another reduction, which appears to be reversible, is observed with $E_{1/2}$ at ca. -1.2 V vs. Ag/AgCl for **3a-c** (Figure 1c); this may be the counterpart of the irreversible process at $E_{p,c} \simeq -1.7$ V vs. Ag/AgCl in the CV of **2**. According to the extended Hückel calculations discussed previously in the case of **2**, both the oxidation and the first reduction processes in complexes **2** and **3** correspond (at least formally) to a change in the bond order from 1 ($\sigma^2\pi^2\delta^{*2}$) to 1.5. However, these are of two distinctly different types, viz. the electron-poor ($\sigma^2\pi^2\delta^{*1}$) and the electron-rich ($\sigma^2\pi^2\delta^{*2}\delta^1$) configurations for the oxidation and reduction, respectively.

As was mentioned earlier in this section, a species of stoichiometry $W_2Cl_5(dppm)_2(CNR)$ may be the precursor to **3** although we were unable to isolate it in pure form from the reaction of **1** with RNC. Also, this same dark brown material (albeit analytically impure) was also obtained in the case of R = xylyl by the chemical reduction (using $(\eta^5\text{-}C_5H_5)_2Co$ in acetone or superhydride in THF) and electrochemical reduction (electrolysis at -0.2 V in 0.2 M TBAH-CH_2Cl_2) of the xylyl isocyanide complex **3b**. There was excellent agreement between the ESR spectra and CV's measured on samples of $W_2Cl_5(dppm)_2(CNxy)$ that were generated both by chemical means and by electrochemical reduction of the cation. The CV of $W_2Cl_5(dppm)_2$-(CNxyl) was identical with that found for the cation of **3b** except that the process at -0.11 V now corresponds to an oxidation. The X-band ESR spectra of frozen solutions of the neutral species in CH_2Cl_2 (-160 °C) exhibit three g values: g_1 = 1.95, g_2 = 1.89, and g_3 = 1.79; g_1 exhibits a phosphorus hyperfine structure ($A \simeq 25$G), but there is no resolvable fine structure associated with either g_2 or g_3 at -160 °C.

The IR spectrum (Nujol mull) of the impure neutral complex has an intense, broad band for $\nu(C{\equiv}N)$ at 2060 cm^{-1}. This represents a shift of 110 cm^{-1} to lower energy from the value of 2170 cm^{-1} found for $\nu(C{\equiv}N)$ in the oxidized complex **3b**. This shift is consistent with the observation in many other systems that π-back-bonding decreases with an increase in metal oxidation state. The decrease of π-back-bonding upon oxidation results in a shift of the $\nu(C{\equiv}N)$ band to higher energy.

In conclusion, we note that the isocyanide-containing species $[W_2Cl_5(dppm)_2(CNR)]^+$ are members of a growing class of multiply bonded dimetal complex that contain π-acceptor CO and RNC ligands and that can be stabilized by intramolecular phosphine bridging ligands.[1-6] Complexes **3a-c** constitute the first such examples for tungsten.

Acknowledgment. We thank the National Science Foundation (Grant No. CHE85-06702) for support of this work. We thank Professor R. E. McCarley for fruitful discussions, for providing us with details of relevant studies underway in his laboratory,[17] and for suggesting alternative strategies for the synthesis of $W_2(\mu\text{-}H)(\mu\text{-}Cl)Cl_4(dppm)_2$. We also thank Professor F. A. Cotton for information concerning the synthesis of $W_2Cl_4(dppm)_2$,[16] Professor T. J. Smith for magnetic susceptibility measurements, and Ju-sheng Qi for experimental assistance.

Supplementary Material Available: Listings of anisotropic thermal parameters (Table S1), bond distances (Table S2), and bond angles (Table S3) and a figure showing the full atomic numbering scheme (Figure S1) (7 pages); a table of observed and calculated structure factors (19 pages). Ordering information is given on any current masthead page.

Contribution from the Department of Chemistry, Purdue University, West Lafayette, Indiana 47907

Binuclear Isocyanide Complexes of Iridium(I). Synthesis, Structure, and Hydrogen Reactivity of $[Ir_2(\mu\text{-}CNR)(CNR)_4(PMe_2CH_2PMe_2)_2][PF_6]_2$ (R = 2,6-$Me_2C_6H_3$, *t*-C_4H_9)

Jianxin Wu, Mark K. Reinking, Phillip E. Fanwick,† and Clifford P. Kubiak*

Received June 17, 1986

The binuclear iridium complexes $[Ir_2(\mu\text{-}CNR)(CNR)_4(PMe_2CH_2PMe_2)_2][PF_6]_2$ (R = 2,6-$Me_2C_6H_3$ (**1**), *t*-C_4H_9 (**3**)) have been synthesized in high yields. Complex **1** crystallizes in the monoclinic space group $P2_1/n$, with a = 19.388 (5) Å, b = 15.193 (5) Å, c = 24.060 (4) Å, β = 94.15 (2)°, and Z = 4. The Ir-Ir separation of 2.7850 (7) Å is consistent with a metal-metal single bond. Complex **1** is fluxional in solution. Variable low-temperature ^1H NMR studies of **1** reveal a dynamic process involving the exchange of isocyanide ligands between bridging and terminal positions. The binuclear iridium(I) complexes, **1** and **3**, react quantitatively with H_2, leading to displacement of one isocyanide ligand and formation of the dihydrides $[Ir_2(\mu\text{-}H)_2(CNR)_4$-$(PMe_2CH_2PMe_2)_2][PF_6]_2$ (R = 2,6-$Me_2C_6H_3$ (**2**), *t*-C_4H_9 (**4**)). Selective ^1H-decoupled ^{31}P NMR experiments have been employed to demonstrate the dihydridic nature of **2** and **4**. The kinetics of the hydrogenation of **1** to **2** has been studied over the temperature range $0 \le T \le 36$ °C. The hydrogenation of complex **1** is first order in [**1**] and zero order in $[H_2]$: $\Delta H^* = 28$ kcal mol^{-1}; $\Delta S^* = 18$ cal mol^{-1} K^{-1}.

We report the preparation of new binuclear isocyanide complexes of iridium bridged by bis(dimethylphosphino)methane (dmpm). The chemistry of mononuclear complexes of Ir has attracted considerable attention becasue of their roles in the activation of C-H bonds,[9-11] CO_2,[12] and H_2.[13] Binuclear com-

†Address correspondence pertaining to crystallographic studies to this author.

(1) Sutherland, B. R.; Cowie, M. *Organometallics* **1985**, *4*, 1637.

0020-1669/87/1326-0247$01.50/0